doi:10.1093/brain/awx320 BRAIN 2018: 141; 271–287 | 271

BRAIN
A JOURNAL OF NEUROLOGY

Widespread brain tau and its association with ageing, Braak stage and Alzheimer's dementia

Val J. Lowe,[1] Heather J. Wiste,[2] Matthew L. Senjem,[1,3] Stephen D. Weigand,[2] Terry M. Therneau,[2] Bradley F. Boeve,[4] Keith A. Josephs,[4] Ping Fang,[1] Mukesh K. Pandey,[1] Melissa E. Murray,[5] Kejal Kantarci,[1] David T. Jones,[1,4] Prashanthi Vemuri,[1] Jonathan Graff-Radford,[4] Christopher G. Schwarz,[1] Mary M. Machulda,[6] Michelle M. Mielke,[2,4] Rosebud O. Roberts,[2] David S. Knopman,[4] Ronald C. Petersen[4] and Clifford R. Jack, Jr[1]

See Herholz (doi:10.1093/brain/awx340) for a scientific commentary on this article.

Autopsy data have proposed that a topographical pattern of tauopathy occurs in the brain with the development of dementia due to Alzheimer's disease. We evaluated the findings of tau-PET to better understand neurofibrillary tangle development as it is seen in cognitively unimpaired and impaired individuals. The evolution of Alzheimer's disease tauopathy in cognitively unimpaired individuals needs to be examined to better understand disease pathogenesis. Tau-PET was performed in 86 cognitively impaired individuals who all had abnormal amyloid levels and 601 cognitively unimpaired individuals. Tau-PET findings were assessed for relationships with clinical diagnosis, age, and regional uptake patterns relative to Braak stage. Regional and voxel-wise analyses were performed. Topographical findings from tau-PET were characterized using hierarchical clustering and clinical characteristic-based subcategorization. In older cognitively unimpaired individuals ($\geqslant$50 years), widespread, age-related elevated tau signal was seen among those with normal or abnormal amyloid status as compared to younger cognitively unimpaired individuals (30–49 years). More frequent regional tau signal elevation throughout the brain was seen in cognitively unimpaired individuals with abnormal versus normal amyloid. Elevated tau signal was seen in regions that are considered high Braak Stage in cognitively unimpaired and cognitively impaired individuals. Hierarchical clustering and clinical characteristic-based categorizations both showed different patterns of tau signal between groups such as greater tau signal in frontal regions in younger onset Alzheimer's disease dementia participants (most of whom had a dysexecutive clinical presentation). Tau-PET signal increases modestly with age throughout the brain in cognitively unimpaired individuals and elevated tau is seen more often when amyloid brain accumulation is present. Tau signal patterns in cognitively unimpaired correspond to early Braak stage but also suggest tangle involvement in extra-medial temporal and extra-temporal regions that are considered more advanced in the Braak scheme even when amyloid negative. Our findings also suggest the possibility of widespread development of early tangle pathology rather than a pattern defined exclusively by adjacent, region-to-region spread, prior to onset of clinical symptoms. Distinct patterns of neurofibrillary tangle deposition in younger-onset Alzheimer's disease dementia versus older-onset Alzheimer's disease dementia provide evidence for variability in regional tangle deposition patterns and demonstrate that different disease phenotypes have different patterns of tauopathy. Pathological correlation with imaging is needed to assess the implications of these observations.

1 Department of Radiology, Mayo Clinic, Rochester, MN, USA
2 Department of Health Sciences Research, Mayo Clinic, Rochester, MN, USA
3 Department of Information Technology, Mayo Clinic, Rochester, MN, USA
4 Department of Neurology, Mayo Clinic, Rochester, MN, USA
5 Department of Neuroscience, Mayo Clinic, Jacksonville, FL, USA
6 Department of Psychiatry and Psychology, Mayo Clinic, Rochester, MN, USA

Received July 26, 2017. Revised October 2, 2017. Accepted October 17, 2017. Advance Access publication December 8, 2017

Correspondence to: Val J. Lowe, MD
Department of Radiology, CH 1-285
Mayo Clinic
200 First Street SW, Rochester, MN 55905
E-mail: vlowe@mayo.edu

Keywords: dementia; tau-PET; Alzheimer's disease; mild cognitive impairment; amyloid-PET

Abbreviations: ADD = Alzheimer's disease dementia; AUROC = area under the receiver operating curve; MCI = mild cognitive impairment; PVC = partial volume correction; SUVr = standardized uptake value ratio

Introduction

Neurofibrillary tangle topographic distribution in the brain is the basis for Braak neurofibrillary tangle pathological staging of Alzheimer's disease (Braak and Braak, 1991). Braak neurofibrillary tangle stage is strongly associated with cognitive impairment (Braak and Braak, 1991; Duyckaerts *et al.*, 1997; Bennett *et al.*, 2004; Sabbagh *et al.*, 2010; Nelson *et al.*, 2012) but shows considerable diagnostic overlap with cognitively unimpaired individuals in autopsy data (Gertz *et al.*, 1996). Some autopsy data of cognitively unimpaired elderly subjects show that neurofibrillary tangle pathology is largely confined to the entorhinal and adjacent temporal isocortices and not often seen in temporal neocortex or extra-temporal regions (Braak and Braak, 1991, 1997; Arriagada *et al.*, 1992; Bouras *et al.*, 1994). Quantification of tau burden during life using PET and ^{18}F-AV-1451 is now possible (Fawaz *et al.*, 2014; Hashimoto *et al.*, 2014; Zimmer *et al.*, 2014) and initial studies show that AV-1451-PET can identify Alzheimer's disease neurofibrillary tangles (Xia *et al.*, 2013*a*). Recent studies have shown that tau-PET closely mimics Braak neurofibrillary tangle staging in Alzheimer's disease (Johnson *et al.*, 2016; Ossenkoppele *et al.*, 2016; Schwarz *et al.*, 2016). In normal ageing, tau-PET signal has been described to occur in the medial temporal lobe, but only in other regions when amyloid is present (Scholl *et al.*, 2016).

Amyloid-PET can identify amyloid-β plaques in the brain (Klunk *et al.*, 2004; Johnson *et al.*, 2007; Clark *et al.*, 2012; Driscoll *et al.*, 2012; Kantarci *et al.*, 2012) and is an important tool for understanding disease pathogenesis and for selecting participants with abnormal amyloid-β for therapeutic trials (Sperling *et al.*, 2014). Soluble oligomeric amyloid-β is hypothesized to be a possible cause of tau hyperphosphorylation and the development of neurofibrillary tangles (Zheng *et al.*, 2002) but the spatial distribution of amyloid and neurofibrillary tangles differ (Okamura *et al.*, 2014). A better understanding of the relationship between tau-PET and amyloid-PET across the spectrum from cognitively unimpaired to cognitively impaired is needed. This study is designed to provide insight on how neurofibrillary tangle pathology might develop in dementia due to Alzheimer's disease (ADD) and how amyloid and neurofibrillary tangles interact in early disease development. Therefore, in this study we evaluated the distribution of tau-PET findings in cognitively unimpaired and cognitively impaired individuals. There were four main aims: (i) assess tau-PET regional uptake as a function of age and other demographics and its ability to distinguish between cognitively unimpaired and cognitively impaired individuals; (ii) determine the influence of amyloid status on regional uptake patterns among cognitively unimpaired; (iii) assess the similarities of tau-PET findings with predicted Braak neurofibrillary tangle stage; and (iv) use clinical groups and clusters of individuals to assess different tau-PET uptake patterns.

Materials and methods

Subjects

Participants were part of the Mayo Clinic Study of Aging or Mayo Clinic Alzheimer's Disease Research Center (Roberts *et al.*, 2008). The Mayo Clinic Study of Aging is a randomized, population-based, ageing study focused on non-demented individuals and encompasses a wide age range. The Mayo Clinic Alzheimer's Disease Research Center is a clinic-based study. There were 601 cognitively unimpaired participants and 86 cognitively impaired participants who completed imaging studies consecutively between 7 April 2015 and 15 February 2017 that were selected. Tau-PET, amyloid-PET and MRI scans were performed in all participants. The participants were determined to be cognitively unimpaired by a consensus diagnosis (this includes quantitative data as well as clinical and cognitive assessment by neurologists, geriatricians, neuropsychologists, and study coordinators). The cognitively impaired individuals were selected if they had amnestic mild cognitive impairment (MCI) or ADD. The diagnosis of MCI was based on published criteria (Petersen, 2004). A diagnosis of dementia was based on the Diagnostic and Statistical Manual of Mental Disorders (American Psychiatric Association, 2000). To increase the likelihood that the cognitively impaired participants were on an ADD pathway, they were required to have abnormal amyloid. In addition, clinical notes for all cognitively impaired participants were reviewed and participants in which an ADD pathway was still unclear (i.e. those without an amnestic component to their presentations) were excluded. After exclusions, 86 participants remained in the cognitively impaired group. No adverse events were seen from imaging.

All participants or designees provided written consent with approval of Institutional Review Boards.

Neuroimaging

For tau-PET, participants were injected with 370 MBq (range 333–407 MBq) of ^{18}F -AV-1451 prior to imaging and imaging was performed as four, 5-min frames for a 20-min PET acquisition, 80–100 min post-injection. Amyloid-PET imaging was performed using Pittsburgh compound B and consisted of four 5-min dynamic frames acquired 40–60 min after injection of 628 MBq (range 385–723 MBq) of ^{11}C-Pittsburgh compound B (PIB) as previously described (Lowe *et al.*, 2014). MRI scans at 3 T with a 3D volumetric T_1 magnetization-prepared rapid gradient-echo sequence were performed as previously described (Murray *et al.*, 2015; Jack *et al.*, 2017).

Image analysis

Cortical regions of interest were defined by an in-house version of the automated anatomic labelling atlas (Tzourio-Mazoyer *et al.*, 2002) as previously described (Vemuri *et al.*, 2008*a*). Non-linear registration using SPM5 (Ashburner and Friston, 2005) was used to apply the atlas to each subject's MRI. The static tau-PET and amyloid-PET volumes were co-registered to the subject's own MRI scan. Statistics on image voxel values were extracted from each labelled cortical region of interest. Individual tau-PET region of interest median values were normalized to cerebellar crus (bilateral crus, 1–2) to calculate regional standardized uptake value ratio (SUVr). The crus region was selected to provide cerebellar grey matter in relative isolation from CSF spaces and to avoid adjacency to parahippocampal, fusiform and lingual gyri to avoid bleed-in signal from tau-pathology. Data with and without partial volume correction (PVC) using the two-compartment method (Meltzer *et al.*, 1999) were evaluated. Global cortical amyloid-PET SUVr was computed from a meta-region of interest normalized to the cerebellar crus where normal or abnormal status was based on a cut-point of 1.42 (Jack *et al.*, 2017).

Statistical methods

The area under the receiver operating characteristic curve was calculated to determine group-wise discrimination performance of tau-PET between cognitively unimpaired and cognitively impaired individuals and between cognitively unimpaired individuals with normal amyloid versus abnormal amyloid. Associations between regional tau-PET SUVr and age were assessed using Spearman rank correlations within cognitively unimpaired individuals with normal and abnormal amyloid, and within cognitively impaired individuals for tau-PET SUVr with and without PVC. Partial correlations were used to assess the associations between tau-PET and age among all cognitively unimpaired individuals, after adjusting for amyloid-PET (using continuous SUVr and without PVC). Correction for multiple comparisons across many regions was performed using permutation-based resampling. For a two-sided family-wise type 1 error of 0.05 across 47 regions, we used a critical value of 2.8 (rather than the usual 1.96) for testing and confidence intervals.

We defined elevated tau-PET in each region based on the 95th percentile among 98 cognitively unimpaired individuals aged 30–49 (all normal amyloid); the 95th percentile was estimated from quantile regression where regions were ordered by median SUVr. We calculated the percentage of individuals with elevated tau-PET for each individual region of interest within cognitively unimpaired abnormal amyloid and normal amyloid individuals aged 50 years or older and cognitively impaired amyloid abnormal individuals. Logistic regression was used to determine if the proportion of cognitively unimpaired individuals with elevated tau-PET was different among the abnormal amyloid compared to the normal amyloid individuals, with and without adjusting for age. Permutation tests were used to determine significant associations after accounting for multiple comparisons. We also defined a group of individuals with intermediate amyloid levels, using the upper tertile of the normal amyloid group (amyloid SUVr of 1.33–1.42, $n = 142$), to assess the percentage of individuals with elevated tau-PET signal. Regions with elevated tau-PET signal were compared to regions in Braak staging.

We used agglomerative hierarchical clustering with Ward's minimum variance method to separately cluster cognitively unimpaired ($\geqslant 30$) and cognitively impaired individuals with similar regional tau-PET findings. Based on the clustering dendrograms, a graphical summary of the dissimilarity between clusters, we chose to group individuals into four cognitively unimpaired and three cognitively impaired clusters by arbitrary visual selection of groupings. Our preliminary findings from the hierarchical clustering suggested different topographical patterns of tau-PET signal. Overall differences in participant characteristics across the four cognitively unimpaired clusters and the three cognitively impaired clusters were assessed with Kruskal Wallis tests for continuous variables and chi-square or Fisher's exact tests for categorical variables. Formal tests of differences in tau-PET among the clusters were not performed since the clusters were defined by tau-PET. Since the number of clusters selected was somewhat arbitrary, we also analysed regional tau-PET findings in *a priori* subcategorizations of the participants into groups based on clinical diagnosis, amyloid-PET status and age as: cognitively unimpaired, normal amyloid <50 years; cognitively unimpaired, normal amyloid $\geqslant 50$ years; cognitively unimpaired, abnormal amyloid $\geqslant 50$ years; amnestic MCI, abnormal amyloid $\geqslant 50$ years; ADD, abnormal amyloid <60 years, ADD, abnormal amyloid 60–70 years; and ADD, abnormal amyloid $\geqslant 70$ years.

To qualitatively assess topographic tau-PET findings, images from participants within each cluster were summed and normalized to produce cluster composite images. Region of interest analyses were performed on clusters and clinical subcategories. Voxel-wise analyses using SPM5 were also performed for clusters and clinical subcategories. Pairwise differences between cluster groups and clinical subcategories were assessed using multiple regression analyses in SPM5 and T-statistic differences between pairs of groups. The results were displayed at a false discovery rate corrected P-value threshold of $P < 0.05$ and no cortical region masking or cluster-based thresholding was performed. The T-statistic group difference maps were transferred to MNI space using spatial normalization (Avants *et al.*, 2008) and from the structural abnormality index (STAND) custom template space to MNI space (Vemuri *et al.*, 2008*b*) and the resulting T-statistic maps were visualized on a 3D rendering with BrainNet-Viewer software (http://www.nitrc.org/projects/bnv/) (Xia *et al.*, 2013*b*).

Results

Cognitively unimpaired and cognitively impaired groups differed by age, *APOE* genotype, Mini-Mental State Examination (MMSE), and tau-PET SUVr (Table 1). Individuals in the cognitively impaired group were required to have abnormal amyloid-PET scans.

Group discrimination

Boxplots of tau-PET by clinical diagnosis showed excellent separation between cognitively unimpaired and cognitively impaired individuals in multiple regions in the brain [area under the receiver operating curve (AUROC) values 0.85–0.94 for many regions] (Supplementary Fig. 1). Tau-PET AUROC values were improved by PVC in 30 of 47 regions ($P \leqslant 0.05$, data not shown). Among cognitively unimpaired, many temporal and extra-temporal tau-PET regions also showed significant discrimination between normal and abnormal amyloid participants (AUROCs 0.60–0.73; 33/47 of regions).

Age associations

Among all cognitively unimpaired, tau-PET SUVr was associated with age in many regions. After adjusting for continuous amyloid-PET, the positive age relationship was seen in only the inferior temporal and amygdala regions (other than non-specific uptake in putamen, pallidum and caudate) (Fig. 1). Amyloid PET in this group was also associated with age and may be difficult to disentangle from a tau-age association (Supplementary Fig. 2). When the cognitively unimpaired normal amyloid and cognitively unimpaired abnormal amyloid groups were analysed separately, most regions showed a positive age relationship with tau-PET SUVr. There were 41/47 regions significantly correlated with age in the normal amyloid cognitively unimpaired group with PVC and 20/47 regions significant without PVC. Age correlations were generally lower without PVC but still significant in several regions. In the cognitively impaired individuals, higher tau-PET SUVr was associated with younger age in most regions. This is likely due to higher tau-PET signal in younger-onset ADD. The putamen and pallidum region values increased with age in all groups and are considered 'off-target' binding (Lowe *et al.*, 2016).

Regional observations of elevated tau-PET signal

Elevated tau-PET SUVr (i.e. tau-PET SUVr above the 95th percentile of young cognitively unimpaired, aged 30–49) was most frequently observed among cognitively unimpaired individuals in the amygdala region (40%), including both abnormal amyloid (55%) and normal amyloid (31%) cognitively unimpaired individuals (Fig. 2). Many other regions, including extra-medial temporal and extra-temporal regions, also had elevated tau-PET among cognitively unimpaired. The high tau-PET SUVr values were seen outside the medial temporal lobe in both temporal and extra-temporal regions in both normal amyloid and abnormal amyloid individuals. The percentage with elevated tau-PET was significantly greater among abnormal amyloid versus normal amyloid cognitively unimpaired in nearly all brain regions. However, after adjusting for age, and correcting for multiple comparisons, this difference remained in only seven regions (Fig. 2, asterisks). In those who had an intermediate level of amyloid (1.33–1.42), two regions more frequently had elevated tau-PET signal in the intermediate

Table 1 Characteristics of participants

Characteristic	Cognitively unimpaired ($n = 601$)	Abnormal amyloid cognitively impaired[a] ($n = 86$)	*P*-value*
Age, years			0.01
Median (IQR)	68 (57, 78)	74 (64, 78)	
Min, max	30, 98	52, 94	
Male gender, *n* (%)	331 (55)	50 (58)	0.59
Education, years, median (IQR)[b]	16 (13, 16)	16 (12, 18)	0.21
APOE ε4 positive, *n* (%)[b]	156 (27)	52 (67)	<0.001
MMSE, median (IQR)[b]	29 (28, 29)	24 (21, 27)	<0.001
Tau-PET, SUVr, median (IQR)[c]	1.07 (1.01, 1.13)	1.64 (1.44, 1.87)	<0.001
Amyloid-PET, SUVr			*
Median (IQR)	1.34 (1.26, 1.46)	2.48 (2.15, 2.69)	
>1.42, *n* (%)	179 (30)	86 (100)	

*P-values are shown for differences between the cognitively unimpaired and cognitively impaired groups. Differences in amyloid-PET were not tested as amyloid-PET was used in defining the groups.

[a]The abnormal amyloid cognitively impaired group includes 35 (41%) individuals with amnestic mild cognitive impairment and 51 (59%) with dementia due to Alzheimer's disease all with amyloid-PET SUVr > 1.42.

[b]Education was missing for one cognitively unimpaired individual; MMSE was missing for four cognitively unimpaired and three cognitively impaired individuals; *APOE* genotype was missing for 28 cognitively unimpaired and eight cognitively impaired individuals.

[c]Tau-PET SUVr is shown for the entorhinal cortex region.

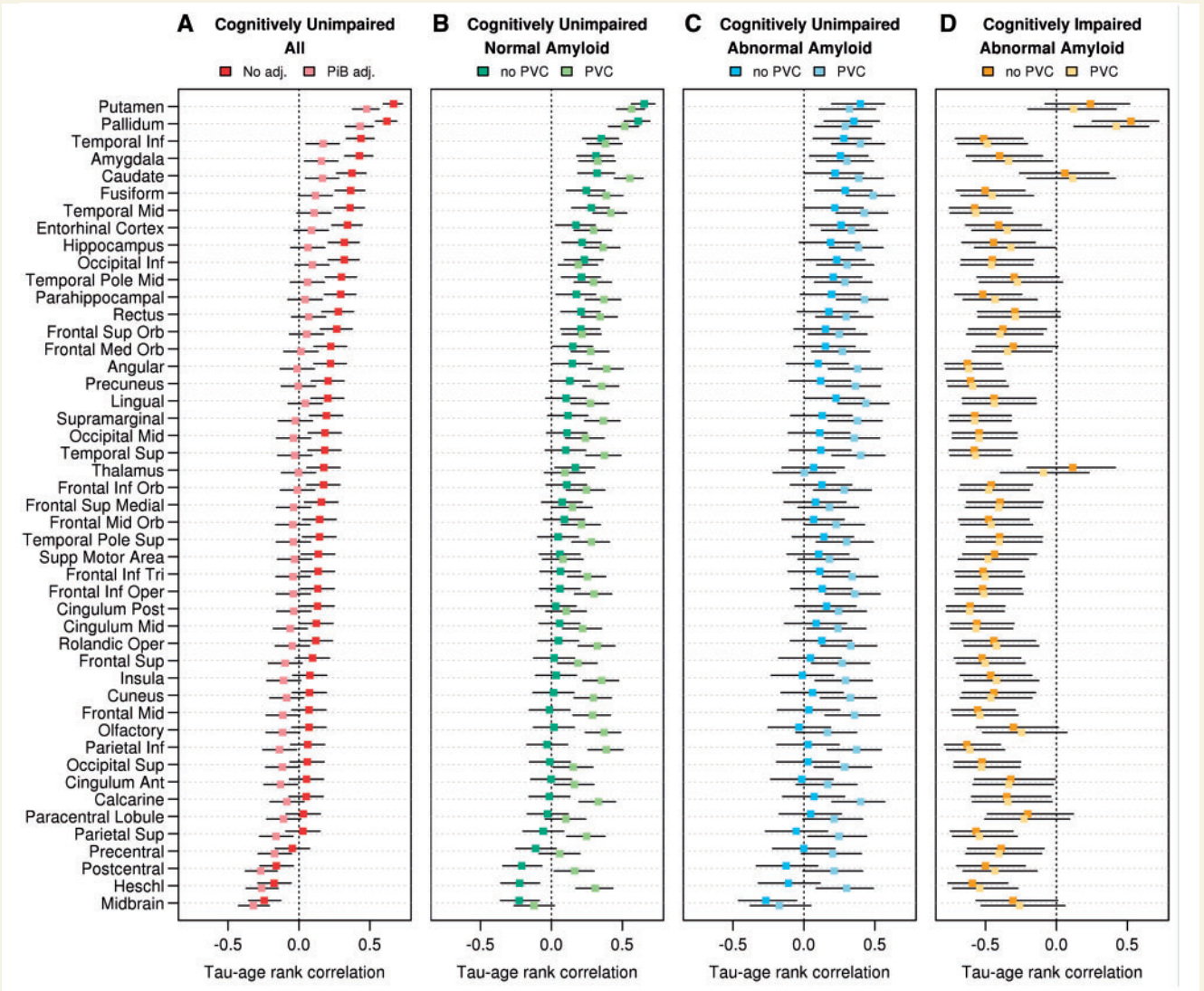

Figure 1 Tau-PET associations with age by region and clinical group. Spearman rank correlation coefficients for the association between regional tau-PET SUVr (without PVC) and age are shown among all cognitively unimpaired individuals in **A** with (light red) and without (dark red) adjusting for amyloid-PET SUVr. Correlations of tau-PET SUVr and age are shown within normal amyloid cognitively unimpaired, abnormal amyloid cognitively unimpaired, and abnormal amyloid cognitively impaired individuals in **B**–**D** for tau-PET values with (lighter colours) and without (darker colours) PVC. Age was significantly correlated with tau-PET among all cognitively unimpaired in 34 of 47 regions without adjusting for amyloid-PET SUVr and in 12 of 47 regions after adjusting for amyloid-PET. Age was significantly correlated with tau-PET without PVC in 20/47 regions among normal amyloid cognitively unimpaired, in 10/47 regions among abnormal amyloid cognitively unimpaired, and in 38/47 regions among abnormal amyloid cognitively impaired. Tau-PET with PVC was associated with age in most regions. Permutation tests were used to correct *P*-values and confidence intervals for multiple comparisons across regions.

group than the low group (amygdala and frontal inferior orbital) and there were no significant regional differences between the intermediate and high PIB groups. All cognitively normal groups have elevated tau-PET signal in regions that were widespread (temporal, frontal superior orbital, inferior occipital, frontal mid orbital, precuneus and others) (Fig. 2 and Supplementary Fig. 3).

Braak staging correlation

The 10 regions (with associated Braak Stage) ranked by the most frequent tau-PET elevation among cognitively unimpaired included the amygdala (Braak Stage III), middle temporal pole (Braak Stage III–IV), inferior temporal (Braak Stage IV), hippocampus (Braak Stage III), entorhinal cortex (Braak Stage I–II), middle temporal (Braak Stage IV), superior frontal orbital (Braak Stage V), rectus (Braak Stage, uncertain), inferior occipital (Braak Stage V), and fusiform (Braak Stage III-IV) (Fig. 2). The entorhinal region ranked fifth in overall frequency; it was tied for eighth in frequency among normal amyloid and was fourth among abnormal amyloid individuals. Examples of the imaging findings are shown on the right in Fig. 2. Tau-PET regions that showed elevated signal

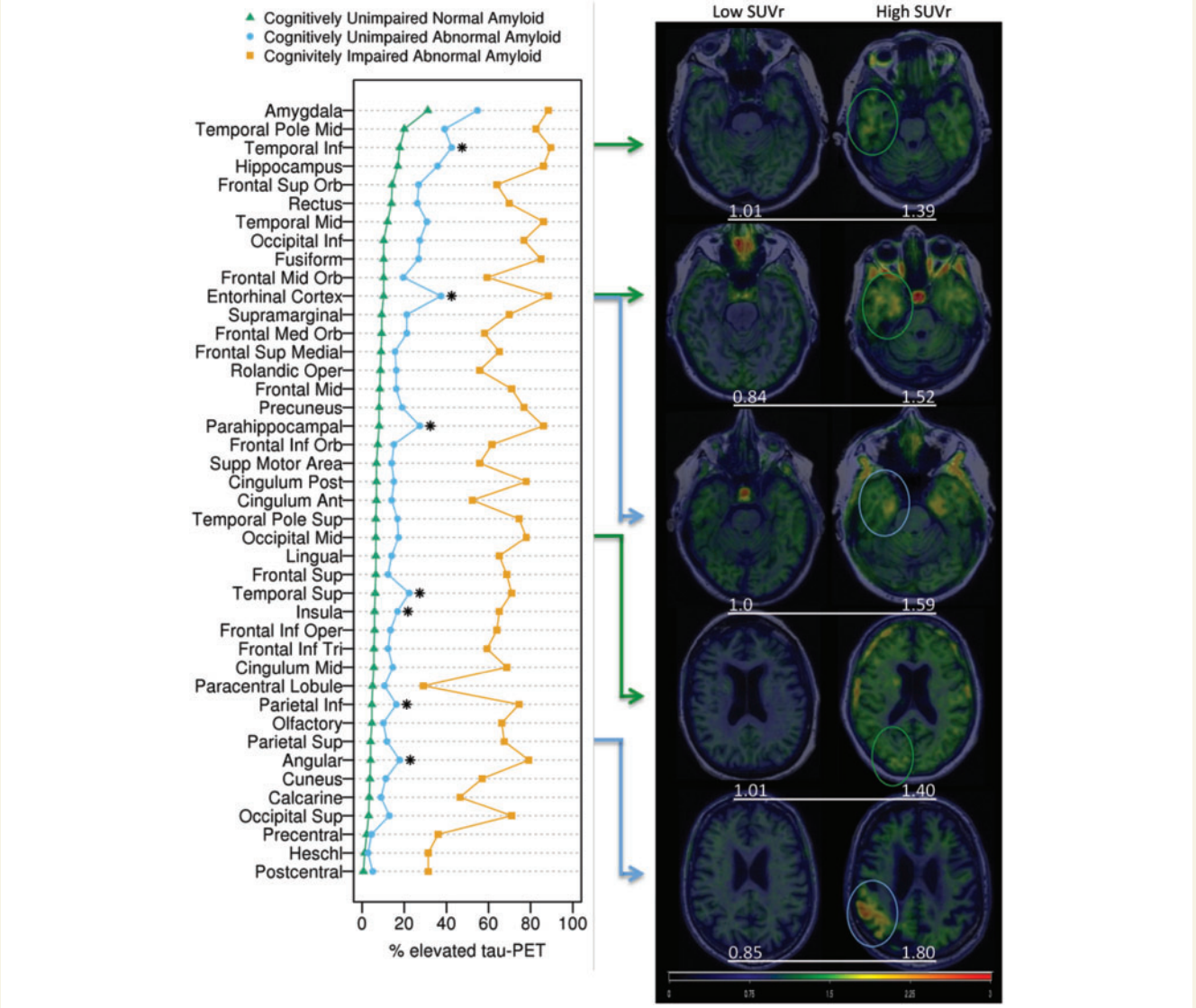

Figure 2 Percentage of individuals with elevated tau-PET signal in each region with image examples. The plot on the *left* shows the percentages of individuals with abnormal tau-PET signal by region within normal amyloid cognitively unimpaired (green), abnormal amyloid, cognitively unimpaired (blue), and abnormal amyloid cognitively impaired (orange) groups. Asterisks indicate regions where the proportion of individuals with elevated tau-PET was significantly greater among abnormal amyloid versus normal amyloid cognitively unimpaired after adjusting for age and correcting for multiple comparisons. Abnormal amyloid cognitively impaired individuals had the higher percentage of elevated tau-PET in all regions. Transaxial tau-PET images shown on the right show low and high SUVr ranges for normal amyloid (green arrows and circles) and abnormal amyloid (blue arrows and circles), cognitively unimpaired participants from selected regions (arrows show the regions that correlate with the images). Three temporal and two extra-temporal regions are shown. SUVr values (white text) are shown below each image. All images are normalized to the same colour scale.

could appear as focal or diffuse accumulations with both abnormal amyloid and normal amyloid individuals and were seen in low and high Braak stage regions in both groups.

Hierarchical clustering

Four cognitively unimpaired clusters and three cognitively impaired clusters were selected by choosing enough distinct clusters while keeping the number of clusters tractable (Supplementary Figs 4 and 5). The demographic characteristics of each cluster are seen in Table 2. Participants within both the cognitively unimpaired and cognitively impaired clusters differed by age. The cognitively impaired clusters also differed by diagnosis, gender, *APOE* genotype, and MMSE. The cognitively unimpaired clusters differed by education, MMSE, and amyloid-PET. Box plots showing selected regional values are shown in Fig. 3 (all regions; Supplementary Fig. 6). Formal tests of differences in tau-PET SUVr across the clusters were not done since the

Table 2 Characteristics of all participants by hierarchical clusters

Characteristic	Among cognitively unimpaired individuals					Among cognitively impaired individuals			
	Cluster 1 (*n* = 33)	Cluster 2 (*n* = 163)	Cluster 3 (*n* = 281)	Cluster 4 (*n* = 124)	*P*-value*	Cluster 1 (*n* = 49)	Cluster 2 (*n* = 31)	Cluster 3 (*n* = 6)	*P*-value*
Diagnosis, *n* (%)					*				<0.001
CU	33 (100)	163 (100)	281 (100)	124 (100)		0 (0)	0 (0)	0 (0)	
aMCI	0 (0)	0 (0)	0 (0)	0 (0)		30 (61)	5 (16)	0 (0)	
ADD	0 (0)	0 (0)	0 (0)	0 (0)		19 (39)	26 (84)	6 (100)	
Age, years					<0.001				<0.001
Median (IQR)	64 (54, 76)	66 (55, 75)	67 (57, 77)	75 (67, 83)		77 (72, 81)	65 (60, 74)	55 (53, 57)	
Min, max	34, 87	30, 98	30, 90	32, 94		61, 94	52, 80	52, 58	
Male gender, *n* (%)	21 (64)	100 (61)	143 (51)	67 (54)	0.13	33 (67)	16 (52)	1 (17)	0.03
Education, years, median (IQR)[a]	14 (12, 16)	16 (13, 17)	16 (13, 17)	14 (12, 16)	0.004	16 (13, 18)	16 (13, 18)	14 (12, 16)	0.50
APOE ε4 positive, *n* (%)[a]	9 (29)	47 (31)	71 (27)	29 (24)	0.58	25 (58)	24 (83)	3 (50)	0.05
MMSE, median (IQR)[a]	29 (28, 29)	29 (28, 30)	29 (28, 30)	29 (28, 29)	0.01	26 (24, 28)	22 (17, 24)	16 (13, 18)	<0.001
Tau-PET, SUVr, median (IQR)[b]	0.92 (0.89, 0.95)	1.00 (0.96, 1.03)	1.08 (1.05, 1.11)	1.20 (1.13, 1.29)	*	1.47 (1.20, 1.68)	1.82 (1.67, 2.00)	1.90 (1.84, 2.01)	*
Amyloid-PET, SUVr									
Median (IQR)	1.23 (1.17, 1.32)	1.31 (1.23, 1.39)	1.35 (1.27, 1.45)	1.39 (1.32, 1.64)	<0.001	2.32 (2.01, 2.70)	2.55 (2.42, 2.69)	2.43 (2.35, 2.53)	0.10
>1.42, *n* (%)	4 (12)	36 (22)	83 (30)	56 (45)	<0.001	49 (100)	31 (100)	6 (100)	*

*P-values are shown for overall tests of any difference in characteristic among the cognitively unimpaired clusters and any difference among the cognitively impaired clusters. Differences in diagnosis among the cognitively unimpaired clusters, tau-PET among the cognitively unimpaired and cognitively impaired clusters, and abnormal amyloid-PET among the cognitively unimpaired clusters were not tested as the clusters were defined using these variables.

[a]Education was missing for one cognitively unimpaired individual; MMSE was missing for four cognitively unimpaired and three cognitively impaired individuals; *APOE* genotype was missing for 28 cognitively unimpaired and eight cognitively impaired individuals.

[b]Tau-PET SUVr is shown for the entorhinal cortex region.

aMCI = amnestic MCI; CU = cognitively unimpaired.

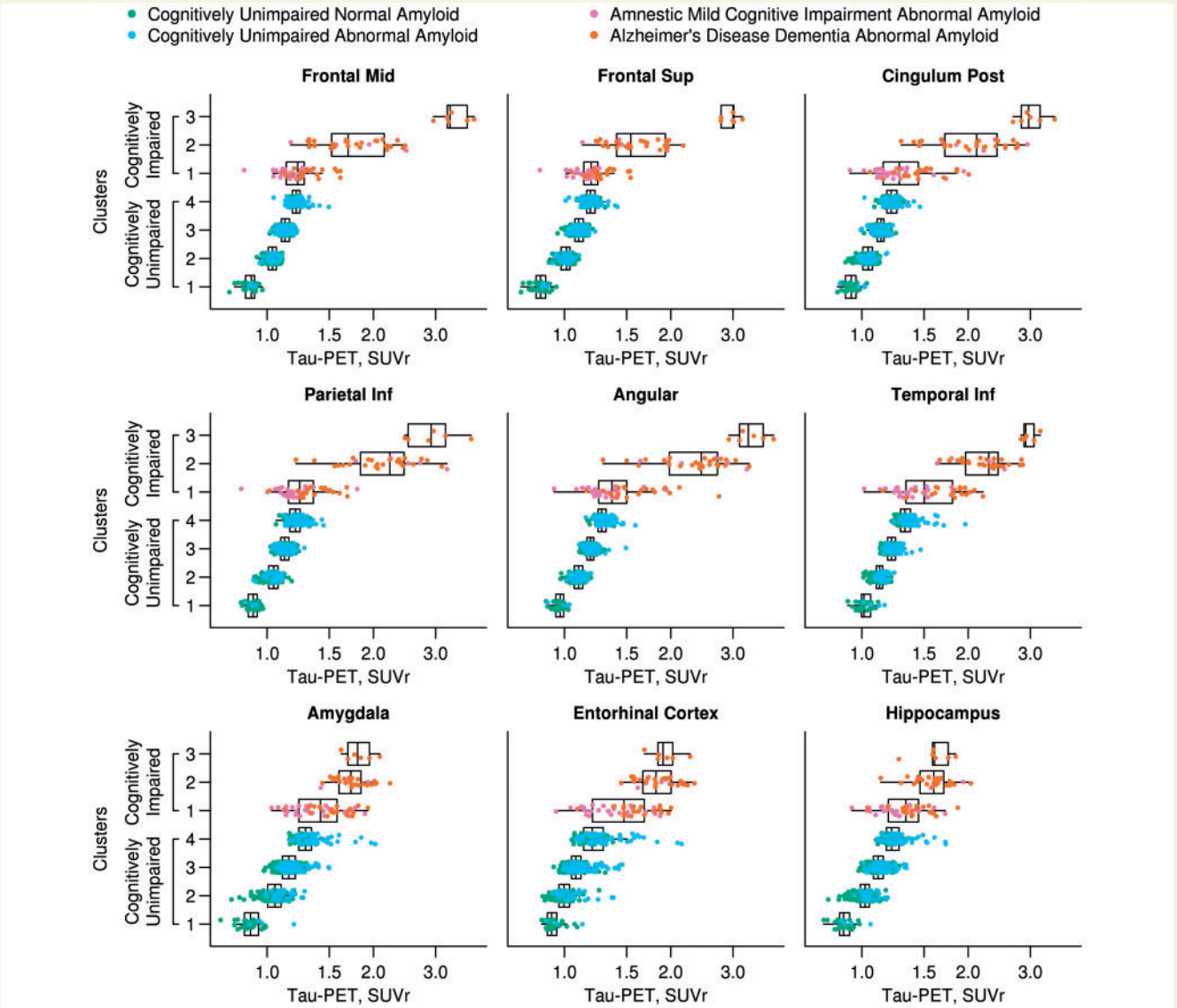

Figure 3 Box plots of regional tau-PET SUVr by hierarchical clusters. Box plots of tau-PET SUVr for nine regions of interest by the four clusters among cognitively unimpaired individuals and three clusters among cognitively impaired individuals. Clinical diagnosis and amyloid-PET status is represented by different colours: normal amyloid cognitively unimpaired, green; abnormal amyloid cognitively unimpaired, blue; abnormal amyloid amnestic MCI (aMCI), purple; abnormal amyloid ADD, orange. The cognitively unimpaired groups have a gradually increasing tau-PET signal in all cortical regions. Greater tau-PET signal is seen in temporal and extra-temporal cortical regions (frontal, posterior cingulate, parietal, angular and temporal inferior) in the cognitively impaired cluster 3 compared to cluster 2 but similar tau-PET signal in the entorhinal cortex was seen in these two groups. Those in the cognitively impaired cluster 1 are more similar to the cognitively unimpaired cluster 4 than the other cognitively impaired clusters. Formal tests of differences in tau-PET among the clusters were not performed since the clusters were defined by tau-PET.

clusters were defined by tau-PET, but visual inspection of the regional tau-PET values show some interesting topographical distributions of tau-PET among the clusters. In the cognitively unimpaired clusters 1 through 4 there was increasing tau-PET signal in all regions. The cognitively unimpaired cluster 4 had similar tau-PET SUVr levels in some regions (frontal, inferior parietal, and posterior cingulate regions for example) to the cognitively impaired cluster 1 group in which there were 61% amnestic MCI and 39% ADD participants. In general, there was a gradient in tau-PET signal across the three cognitively impaired clusters with $1 < 2 < 3$. Cluster 3 was the smallest cluster, younger, all were ADD, and had visually different topographical distributions of tau-PET signal. In particular, cluster 3 had higher tau-PET SUVr in many regions compared to the other cognitively impaired groups with examples shown in Fig. 3 as mid-frontal, superior frontal, posterior cingulate, inferior parietal, angular, and inferior

temporal regions (AUROC 0.89–1.0). This was in contrast to other regions such as the medial temporal regions (amygdala, entorhinal cortex and hippocampus shown) where the SUVr were more similar between cluster 3 and cluster 2 (AUROC 0.54–0.65).

Clinical characteristic subcategorization

A priori grouping of participants by clinical diagnosis, age, and amyloid-PET abnormality showed tau-PET signal increasing from cognitively unimpaired normal amyloid to cognitively unimpaired abnormal amyloid and from amnestic MCI to ADD individuals. Differences in tau-PET SUVr were seen among the three cognitively unimpaired groups and among the four cognitively impaired groups for all nine regions shown in Fig. 4 ($P < 0.01$ after adjusting for multiple comparisons). Variation in tau-PET signal across cognitively impaired groups was comparable to hierarchical clustering with tau-PET signal being appreciably higher in extra-temporal regions for younger versus older-age cognitively impaired individuals (Fig. 4 and Supplementary Fig. 7).

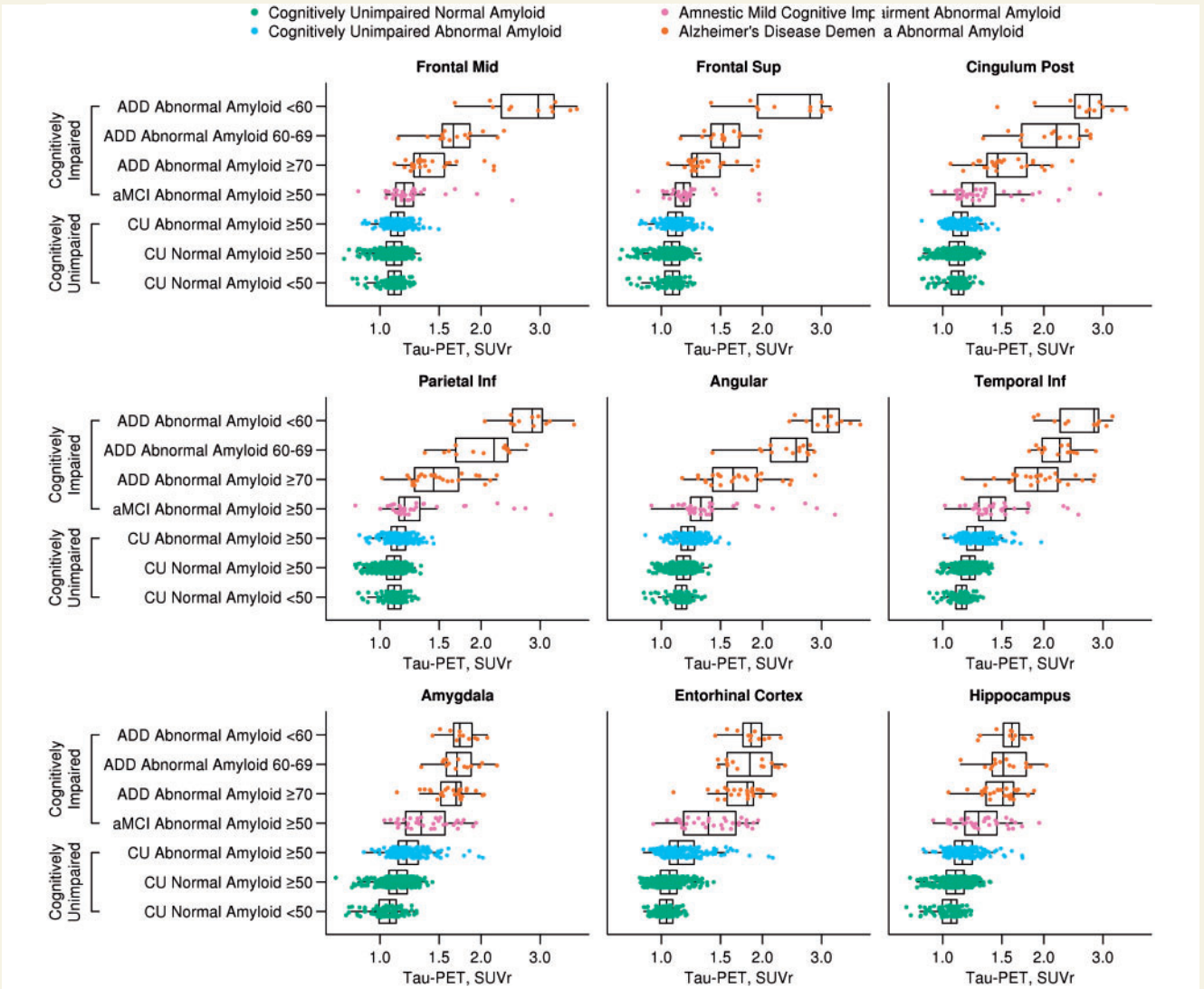

Figure 4 Box plots of regional tau-PET SUVr by age, amyloid-PET status and diagnosis subcategorization. Box plots of tau-PET SUVr for nine regions of interest by clinical diagnosis, amyloid-PET status, and age. Clinical diagnosis and amyloid-PET status are represented with different colours: normal amyloid cognitively unimpaired, green; abnormal amyloid cognitively unimpaired, blue; abnormal amyloid amnestic MCI (aMCI), purple; abnormal amyloid ADD, orange. Tau-PET SUVr differed significantly ($P < 0.01$), after adjusting for multiple comparisons, among the three cognitively unimpaired groups and among the four cognitively impaired groups for all nine regions shown in the figure. There is greater tau signal in the medial and extra medial temporal regions (inferior temporal for example; other regions seen on Supplementary Fig. 7) than in the cognitively unimpaired >50 normal amyloid group versus the cognitively unimpaired normal amyloid <50 group. The box plots also show a similar pattern of increased tau-PET signal in younger age ADD as compared to the cluster analysis with much higher extra-temporal tau-PET signal. However, there are participants in the younger age ADD group with tau-PET signal similar to the older age ADD group.

In contrast, medial temporal tau-PET signal (entorhinal and hippocampal regions for example) was more similar between younger and older cognitively impaired individuals (<60 versus ⩾70 ADD) in the clinical subcharacterization. The amnestic MCI group generally had lower tau-PET signal than the ADD groups; however, there were a number of amnestic MCI individuals with very high tau-PET SUVr in some regions (angular and parietal regions, for example). The cognitively unimpaired groups showed less variation in magnitude of tau-PET signal across regions than what was seen in the hierarchical clustering. In the hierarchical clustering, several cognitively unimpaired normal amyloid participants are clustered with cognitively unimpaired abnormal amyloid individuals (e.g. green dots in the cognitively unimpaired cluster 4 in the posterior cingulate, parietal and angular regions, Fig. 3) and are also similar in tau-PET SUVr to cluster 1 cognitively impaired individuals. The hierarchical clustering may be better at identifying cognitively unimpaired individuals with possible preclinical Alzheimer's disease tau-PET signal patterns (e.g. cognitively unimpaired cluster 4 individuals) than simply grouping cognitively-unimpaired individuals by age and amyloid abnormality.

Voxel-wise analyses

The voxel-wise image data are displayed as summed image data from each individual cluster for a descriptive display (Supplementary Fig. 8) and as contrasts between the clusters to descriptively show tau-PET signal differences (Fig. 5). As the clustering used tau-PET SUVr to identify groups with similar tau patterns, the reported T-statistic in the colour bar for the contrasts in these clusters is descriptive. Cognitively unimpaired clusters topographically look similar with greater widespread brain tau-PET signal progressing from cognitively unimpaired cluster 1 to cognitively unimpaired cluster 4 on the summed data. Greater diffuse temporal and parietal tau-PET signal is visible on the summed images in cognitively unimpaired cluster 4 or cognitively unimpaired cluster 3 and is seen on the SPM contrast as well. On SPM analyses, more contrast between cognitively unimpaired cluster 2 and cognitively unimpaired cluster 1 is seen in the frontal regions and continues to be a prominent finding in the other cognitively unimpaired cluster contrasts. Differences are seen in many other regions of the brain between the cognitively unimpaired clusters. Cognitively impaired cluster 3 (mostly younger-age onset ADD) had the highest levels of tau-PET across most regions on the region of interest analysis and has greater tau-PET signal contrast in the frontal, temporal, parietal, posterior cingulate and angular regions as compared to other cognitively impaired clusters. Interestingly, there was relative sparing of incremental tau-PET signal in medial temporal regions in cognitively impaired cluster 3 as compared to cognitively impaired cluster 2 or cognitively impaired cluster 1. Cognitively impaired cluster 2 has higher tau-PET signal compared to cognitively impaired cluster 1 in the temporal, parietal and posterior cingulate regions.

The voxel-wise image data for the clinical-characteristic groups are displayed as contrasts to show significant differences in tau-PET signal between the groups (Fig. 6). In normal amyloid, cognitively unimpaired older participants, greater medial temporal, extra-medial temporal and basal frontal tau-PET signal was seen than in younger normal amyloid, cognitively unimpaired participants. Amnestic MCI participants had greater temporal, parietal, posterior cingulate and frontal tau-PET signal than cognitively unimpaired participants. Similar to the clustering findings, in the clinically subcategorized group contrasts, younger ADD show greater contrast of tau-PET signal and more frontal tau-PET signal with medial temporal sparing than older ADD.

Tau patterns and relationship with clinical phenotypes

The clinical phenotypes of the cognitively impaired clusters differed. In the cognitively impaired cluster 3, 5/6 had the rare dysexecutive phenotype of ADD while 1/6 was described as younger-age onset, memory-predominant ADD. The SPM analysis and region of interest analyses showed more tau-PET signal in the frontal regions in the cognitively impaired cluster 3. Interestingly, in the cognitively impaired cluster 2, 3/31 were called dysexecutive ADD and another one had a mild mixed memory and dysexecutive presentation. Other individuals in cluster 2 were either MCI or ADD, of which additional clinical findings of sleep apnoea ($n = 1$), topographical agnosia ($n = 1$), and limbic ADD ($n = 1$) were seen. The dysexecutive ADD individuals in cognitively impaired cluster 2 had less frontal tau signal than those in cluster 3 on visual inspection (data not shown), consistent with the clustering results. The cognitively impaired cluster 3 participants had the lowest MMSE.

Discussion

Determining the distribution of neurofibrillary tangles across the lifespan is important to better elucidate the sequential evolution of the pathophysiology of ADD. In this study we used tau-PET to infer the regional characteristics of neurofibrillary tangles seen in cognitively unimpaired and cognitively impaired individuals and correlated topographical tau-PET patterns with clinical diagnosis, age, and amyloid status. We emphasize four major findings. First, tau-PET SUVr was modestly associated with age throughout most regions of the brain in cognitively unimpaired individuals. Second, this widespread elevated tau-PET signal in the brain was seen in both normal amyloid and abnormal amyloid status, cognitively unimpaired individuals (i.e. signal was not confined to medial temporal regions). Third, the distribution of tau-PET signal in

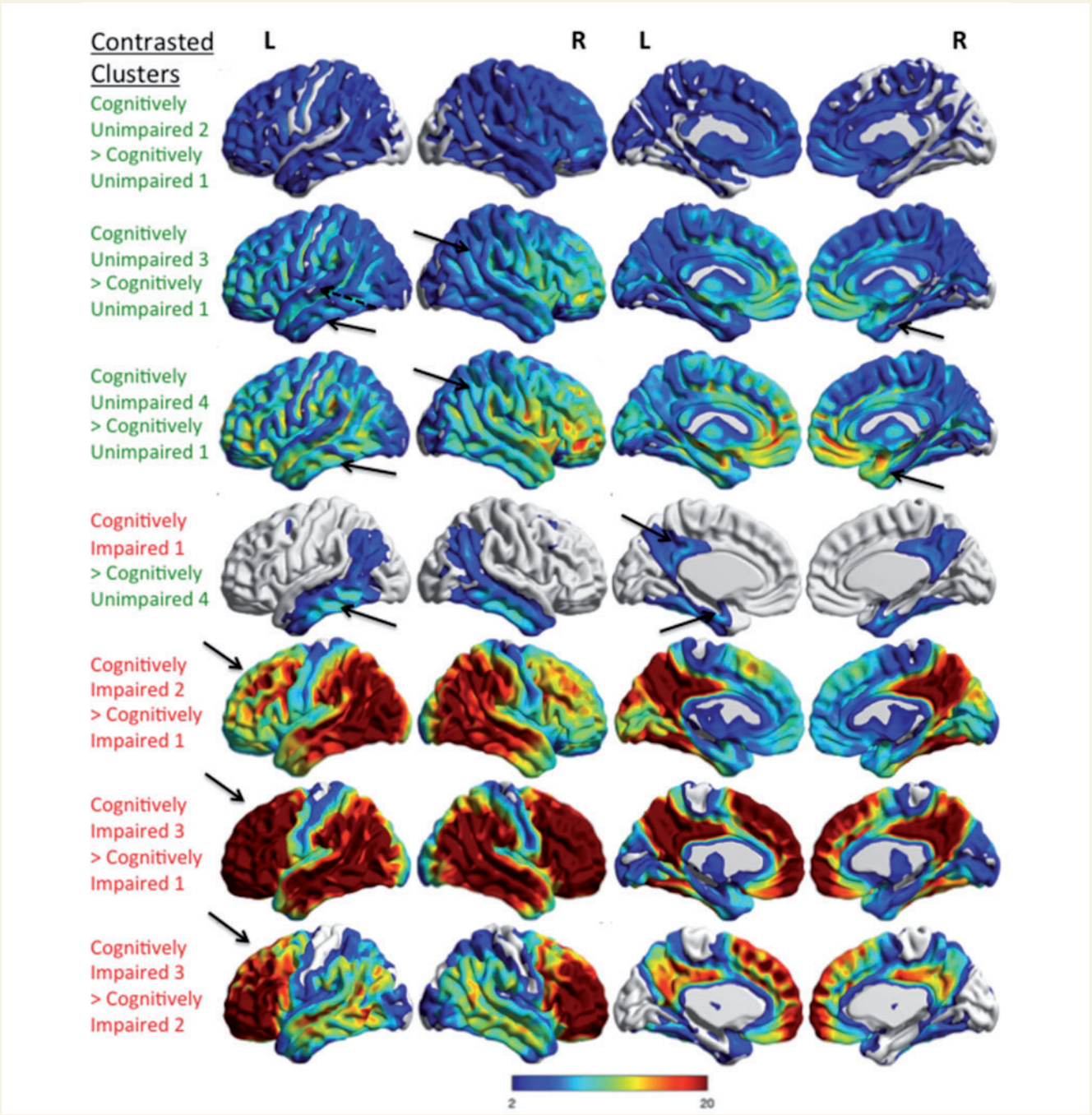

Figure 5 Comparison of the differences in tau-PET signal between hierarchical clusters. Voxel-wise tau-PET findings that are greater between pairs of hierarchical clusters are shown. The upper three rows show the comparisons of cognitively unimpaired clusters (green text). The lower four rows show cognitively impaired cluster comparisons (red text). There is greater tau-PET signal diffusely in cognitively unimpaired 2 versus cognitively unimpaired 1 clusters. Greater tau-PET signal is seen in cognitively unimpaired 3 and cognitively unimpaired 4 versus cognitively unimpaired 1 in the whole temporal and parietal lobes (arrows). Frontal accumulation is incrementally greater also. The incremental tau-PET signal seen between the different cognitively unimpaired clusters involves many regions of the brain outside of the temporal lobe. The magnitude of the increased tau-PET signal in the cognitively impaired clusters is greatest in the frontal lobes and is similar to the findings in Fig. 3. The cognitively impaired cluster 1 shows increased inferior temporal, medial temporal and posterior cingulate tau-PET signal (arrows) as compared to cognitively unimpaired cluster 4. Greater tau-PET signal in cognitively impaired 2 versus cognitively impaired 1 is seen in the temporal, parietal and posterior cingulate regions and less so in the frontal lobe (arrow). Cognitively impaired cluster 3 showed greater tau-PET signal in the frontal, temporal, parietal, posterior cingulate and angular regions than cognitively impaired 1 or cognitively impaired 2 clusters with pronounced increase in the frontal lobe versus cognitively impaired cluster 1 (arrows). All results were family-wise error (FWE) corrected, $P < 0.05$ and the colour bar shows the T-statistic range for all contrasts but is descriptive as the clustering was defined by using tau-PET SUVr.

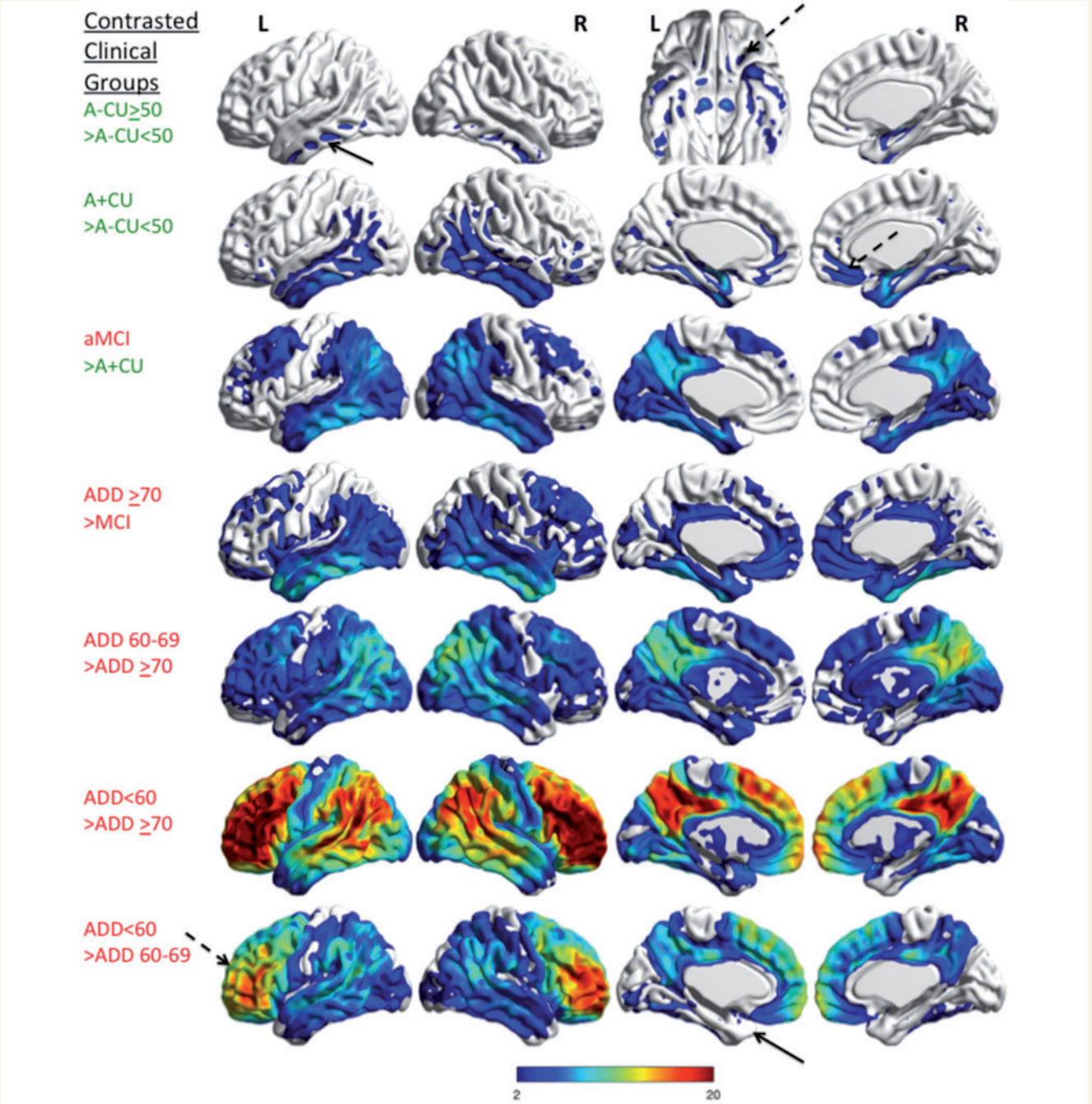

Figure 6 Comparison of the differences in tau-PET signal between clinically characterized groups. Voxel-wise tau-PET findings that are greater between pairs of the clinically characterized groups are shown. The upper two rows show the comparisons of cognitively unimpaired groups by age and amyloid status (green text). The lower five rows show comparisons of cognitively impaired groups by diagnosis comparisons (red text). There is greater tau-PET signal in the inferior temporal lobes (black arrow) (in additional to medial temporal lobes) and frontal orbital regions (dashed arrow, shown on inferior view) in the cognitively unimpaired >50 normal amyloid group versus the cognitively unimpaired normal amyloid <50 group. Greater tau-PET signal is seen in the temporal, parietal and the frontal lobes (dashed arrow) in the cognitively unimpaired abnormal amyloid group versus the cognitively unimpaired normal amyloid <50 group. The amnestic MCI group shows increased temporal, parietal, posterior cingulate, and frontal tau-PET signal as compared to the cognitively unimpaired abnormal amyloid group and a similar pattern is also seen in ADD ⩾70 versus amnestic MCI. This pattern is seen in ADD 60–69 versus ADD ⩾70 but is more diffuse. When the ADD <60 is contrasted to the other ADD groups, incremental frontal tau-PET signal is prominent (dashed arrow) but medial temporal differences are relatively small (arrow). All results were few corrected, $P < 0.05$ and the colour bar shows the T-statistic range for all contrasts. A = amyloid; aMCI = amnestic MCI; CU = cognitively unimpaired.

cognitively unimpaired individuals suggested a pattern of early neurofibrillary tangle deposition with similarities to Braak neurofibrillary tangle staging but also with exceptions. And fourth, regional hierarchical clustering of tau-PET signal and clinical characteristic-based grouping of individuals revealed variable patterns of neurofibrillary tangle topographical distributions within cognitively unimpaired and cognitively impaired subgroups. These four observations demonstrate common principles of the pathophysiology of ADD: namely that neurofibrillary tangle abundance is in part an ageing phenomenon; that β-amyloidosis may be a trigger to neurofibrillary tangle progression but widespread, low level tangle deposition can occur in the absence of amyloidosis, and that regional expansion of increasing neurofibrillary tangle burden begins during the preclinical phase of the disease and that neurofibrillary tangle topographical distribution in the brain can have clinical relevance in impaired individuals.

With our large sample size, we were able to detect a significant, but modest age relationship with tau-PET signal in many regions of the brain among (i.e. not just medial temporal) cognitively unimpaired individuals. In a prior tau-PET study, the association between increasing age and higher tau-PET among 38 cognitively unimpaired participants was limited to the medial temporal structures, ventral frontal cortex and insula (Scholl *et al.*, 2016). In other studies, age was not associated with tau-PET signal (Brier *et al.*, 2016; Schwarz *et al.*, 2016). In one recent study, tau-PET signal was not seen outside of the medial temporal lobe in normal amyloid, cognitively unimpaired older adults ($n = 58$, >50 years) as compared to younger adults (Pontecorvo *et al.*, 2017). In contrast, our tau-PET findings in a larger cognitively unimpaired group, showed age-associated tau-PET signal in most regions of the brain—whether individuals had normal or abnormal amyloid status. The observed broader brain distribution of age-related, tau-PET signal in cognitively unimpaired participants seen in our group may differ from prior reports because of the size of our population, our recruitment methods (the cognitively unimpaired group is from a population-based sample), or image analysis methodological differences. Importantly, for image analyses, we defined abnormal tau-PET signal as being greater than that seen in a group of young cognitively unimpaired individuals (<50 years of age) and the definitions of abnormality are specific for each region rather than for a meta-region of interest or a large brain region. This has some contrasts to prior reports that used multi-region-composite regions, often designed to mimic Braak stage regional anatomy (Johnson *et al.*, 2016; Scholl *et al.*, 2016; Schwarz *et al.*, 2016).

Regional tau-PET signal in the cognitively unimpaired group was shown with and without adjustment for continuous amyloid-PET SUVr. It is difficult to disentangle the effects of amyloid on tau-PET signal as amyloid also has an age relationship in the population (Jack *et al.*, 2014). After adjustment for amyloid-PET, the positive tau-PET age associations were limited to inferior temporal and amygdala regions. Interestingly, in the combined cognitively unimpaired group, some regions were also negatively correlated with age after adjusting for amyloid-PET SUVr. This may be due to an over-correction or be an artefact of the analysis, or could be explained if the older abnormal amyloid individuals were 'resilient' to amyloid (i.e. remained cognitively unimpaired rather than progressing to dementia) and had less tau than younger abnormal amyloid individuals (Fig. 1A). In support of this idea, when abnormal amyloid and normal amyloid groups were analysed separately, positive age correlation was seen in most regions. Extra-temporal tau-PET signal in normal amyloid, cognitively unimpaired older adults—similar to our findings—may have been subtly present in prior work, but was not specifically discussed [see Fig. 1 in Scholl *et al.*, (2016), with older normal amyloid individuals showing diffuse tau-PET signal greater than the younger group]. Interestingly, in our cognitively impaired group, higher tau SUVr was associated with younger age in most regions. This could be explained by younger-onset probable ADD (cognitively impaired cluster 3) having more severe tau burden versus older-onset participants and is consistent with our cluster findings (Table 2 and Fig. 5).

We evaluated the percentage of individuals with elevated tau-PET signal in each region among cognitively unimpaired individuals with normal and abnormal amyloid status and found that elevated tau-PET signal was seen frequently in medial temporal lobe regions but also in many extra-temporal brain regions among those with either normal or abnormal amyloid status (Fig. 2). This contrasts with previous reports where participants with normal amyloid were said to have no tau-PET signal elevation outside of the medial temporal lobe (Scholl *et al.*, 2016). Most regional elevations showed a trend of being more frequent in cognitively unimpaired participants with abnormal amyloid, with some ($n = 7$) still significantly more frequent than those with normal amyloid after correction for multiple comparisons and age. These regional tau-PET findings have similarities to Braak descriptions of early neurofibrillary tangle extent, but are not identical, with some elevated tau-PET regions being located in Braak Stages III–VI areas. This was true for tau-PET signal in both normal and abnormal amyloid, cognitively unimpaired participants and would suggest that high Braak Stage (extra-medial temporal and extra-temporal neocortex) deposition can occur independent of amyloid. These findings could be concordant with primary age-related tauopathy (PART) (Crary *et al.*, 2014) and with our own pre-tau PET observations in persons with a suspected non-Alzheimer pathophysiology (SNAP) designation (Knopman *et al.*, 2013). These findings are supported by prior autopsy and tissue data. In Braak's 1996 publication (Braak *et al.*, 1996), amyloid deposition did not always precede neurofibrillary tangle deposition. Importantly, the neurofibrillary tangles in PART is 3R/4R and should be identified by tau-PET. We have previously demonstrated binding of

AV-1451 to PART tau by autoradiography as compared to immunohistochemistry (Lowe *et al.*, 2016). Together, these data provide biomarker evidence to suggest that PART, commonly thought to be mostly restricted to the medial temporal lobe and other allocortical areas, or some other cause of tau-PET signal elevation without amyloid, is a relatively common finding in cognitively unimpaired and could be more widespread in the brain than previously thought. Its clinical significance, however, remains uncertain and correlation with the development of cognitive impairment, longitudinal data and clinicopathological verification will be needed to further understand its importance. Indeed we recently found poorer cognitive performance and atrophy of the head of the left hippocampus in participants with PART suggesting PART may not be a silent pathology (Josephs *et al.*, 2017).

Two recent studies reported increased tau-PET only in medial temporal or temporal structures in groups of 15 and 56 cognitively unimpaired individuals, respectively (Johnson *et al.*, 2016; Ossenkoppele *et al.*, 2016). Furthermore, extra-temporal neurofibrillary tangle findings are not highlighted in some large ageing population autopsy studies (Braak and Braak, 1997). These differences from our findings could be partially explained by the tissue sampling limitations inherent in autopsy studies and possibly the smaller sample sizes in previous tau-PET studies. Our tau-PET findings suggest that high Braak neurofibrillary tangle stages may be frequently detected by tau-PET in cognitively unimpaired subjects. Supportive of these PET findings are smaller cohort autopsy data showing that: (i) advanced neurofibrillary tangle stages (IV–VI) are seen in cognitively unimpaired and demented individuals with considerable overlap (Gertz *et al.*, 1996); (ii) widespread isocortical neurofibrillary tangles were 'less frequent' but present in cognitively unimpaired (Arriagada *et al.*, 1992); (iii) 'a few scattered' neurofibrillary tangles are clearly seen in the isocortex in cognitively unimpaired (Braak and Braak, 1991); and (iv) only small numbers of normal ageing and ADD patients conform in all respects to Braak neurofibrillary tangle hierarchy (Gertz *et al.*, 1998). In addition, autopsy data also support progressive increase in neurofibrillary tangle frequency with age in limited regions (Braak *et al.*, 1996). In concordance with earlier autopsy data, the magnitude of tau-PET SUVr values among cognitively unimpaired was relatively low compared to cognitively impaired, suggesting that modest neurofibrillary tangle involvement as suggested by tau-PET is a reasonable correlate to autopsy data (Arriagada *et al.*, 1992). Importantly, quantitative analysis of neurofibrillary tangles has shown neurofibrillary tangle density/mm^2 in the superior frontal cortex to be 4.9 ± 0.5 versus 7.7 ± 3.3 in cognitively unimpaired versus ADD (a relatively modest difference), and in layer II of the entorhinal cortex to be 7.4 ± 0.8 versus 59.1 ± 12.4 in cognitively unimpaired versus ADD (Bouras *et al.*, 1994). Together, these autopsy data support fewer, but not absent, neurofibrillary tangles in extra-temporal and temporal regions in cognitively unimpaired versus ADD at the time of autopsy, consistent with the findings on tau-PET of an increasing presence of neurofibrillary tangles throughout the brain with ageing.

The biological significance of widespread tau-PET signal in abnormal amyloid and normal amyloid cognitively unimpaired individuals is unknown. The medial temporal elevations seen in cognitively unimpaired cluster 4 could represent a classic appearance of pathology that could be expected to lead to ADD. Further longitudinal imaging and follow-up will be needed to determine with any certainty the significance of these findings. Nevertheless, these tau-PET findings provide observations that could add important insight to the biology of neurofibrillary tangle development in Alzheimer's disease and direct subsequent studies. Some current thinking suggests a topographical progression of neurofibrillary tangle, possibly facilitated by trans-synaptic spread of misfolded tau protein (Guo and Lee, 2011). Trans-neural spread through network connections could facilitate this propagation to distant areas within a functional network (Stancu *et al.*, 2015). The tau-PET data presented herein support the development of widespread, age-related neurofibrillary tangles in the brain. This could be a manifestation of trans-neuronal spread but at an age years before symptomatic disease. Worsening of neurofibrillary tangle pathology, associated with a trigger, possibly amyloid and/or neural network-related activity, could potentially lead to progressive neurofibrillary tangle pathology that eventually causes clinical symptoms. Additional recent observations show that soluble phosphorylated high molecular weight tau, found in the extracellular space, can trigger tau propagation, and provide supporting biochemical data of another hypothesis of how widespread tau development throughout the brain could occur (Takeda *et al.*, 2015). These ideas of tau spread to distant, non-adjacent brain regions may be consistent with our findings. Widespread tau propagation could provide the milieu for further neurofibrillary tangle development, again with the aid of other triggers like amyloid and/or neural network-related activity, in more specific, disease-related regions. Our data show that age-related, widespread elevated tau-PET signal becomes more frequent and of greater magnitude when amyloid is elevated and supports these ideas. Longitudinal and clinical–pathological validation studies are needed to evaluate these hypotheses.

Findings from the clustering analyses and subcategorization by clinical findings provided several important insights. The clustering analyses defined three cognitively impaired groups and demonstrated that younger-age onset ADD had more diffusely distributed and higher tau-PET SUVr signal with some cortical region preferences (e.g. frontal regions, posterior cingulate, and parietal regions being greater) as compared to older-age onset ADD. The cognitively impaired clusters differed by age, diagnosis, gender, and *APOE* genotype status suggesting clinically relevant implications of the tau-PET patterns. Medial temporal regions were also relatively spared in the younger-age onset cognitively impaired cluster relative to the other cognitively

impaired clusters. In the cognitively impaired cluster 3, 5/6 had a dysexecutive phenotype of ADD while 1/6 was described as younger-age onset ADD. Behavioural or dysexecutive ADD is a rare ADD phenotype in which clinical-anatomic correlations are poorly understood. Previous work has shown that this group has some biomarker differences (atrophy on MRI) as compared to behavioural variant frontotemporal dementia (Ossenkoppele *et al.*, 2015). Differences in glucose metabolism and amyloid distribution in younger onset ADD as compared to older onset ADD have also been described in prior studies that showed more parietal abnormalities in younger onset ADD (Ossenkoppele *et al.*, 2012, 2015). The clustering method we used grouped mostly dysexecutive ADD phenotype participants in a single cluster while the clinically based subcategorization included five other individuals in the ADD <60 year-old group. These five individuals in the clinically based subcategorization did not have highly elevated frontal tau-PET signal (two of whom had a dysexecutive phenotype) as seen in the cognitively impaired cluster 3 (on visual review) and were included in other clusters by the clustering method. While the numbers are too small to be definitive, the finding suggests that topographical tau-PET distribution may be helpful in younger onset ADD phenotype characterization and that different regional patterns of tau-PET signal are associated with different ADD phenotypes. Future work in non-amnestic ADD patients and in persons with other non-Alzheimer's disease-tauopathies will be important to assess the variability of tau topographical distributions that may be present in the tau-disease spectrum.

We hypothesized that the clustering analysis would detect groups of individuals with distinct regional patterns of tau-PET signal and particular phenotypes in the cognitively unimpaired group similar to how it performed in the cognitively impaired group. Increasing tau-PET signal was seen globally in cognitively unimpaired clusters 1 through 4 and we saw greater temporal and parietal tau-PET signal in the highest tau-PET signal cognitively unimpaired clusters. We may not have been able to detect additional patterns in cognitively unimpaired individuals possibly because our cognitively unimpaired cluster groups were large and not granular enough to detect early development of specific ADD or atypical ADD phenotypes. It will be interesting to see in the future if defining tau-PET topographically associated groups by other clustering selections or other clinical methods will be better at identifying tau patterns that can predict ADD phenotypes in preclinical stages.

Lastly, highly accurate group-wise separation of cognitively unimpaired and cognitively impaired groups with tau-PET was seen using almost any cortical region of the brain. Similar findings by others have been seen in limited regions (Johnson *et al.*, 2016; Ossenkoppele *et al.*, 2016; Schwarz *et al.*, 2016). While medial temporal regions had some of the highest tau-PET SUVr and AUROC values, high discriminative ability was seen throughout most brain regions. Our data support prior findings with the addition of widespread brain tau-PET signal also being able to discriminate abnormal amyloid and normal amyloid, cognitively unimpaired groups.

Limitations include tau-PET signal in off-target sites. We have previously shown that tau-PET signal can be seen in off-target sites and other non-tauopathies (Lowe *et al.*, 2016). For example, retention in the choroid plexus could bias medial temporal lobe regional findings. We think that this influence is likely minimal as we found that only four cases in the cognitively unimpaired group had elevated tau signal only in the entorhinal cortex of the medial temporal lobe regions and only 1/4 had abnormal entorhinal cortex tau-PET signal as the sole finding. Two of these four were unlikely to have a choroid plexus bias because low choroid plexus retention was seen visually. This demonstrates that choroid plexus 'bleed in' is likely of limited importance in group-wise analyses. We also showed that entorhinal cortex tau-PET signal has significant clinical relevance in region of interest analysis (Fig. 4) supporting the idea of limited bias. We also selected a group of participants aged <50 to determine tau-PET 'normality.' Early tau deposition may be present in some younger participants. In any case, this would likely conservatively bias our results. Autopsy data correlated with ante-mortem imaging and longitudinal comparisons will be needed for verification of the implications of age-related or widely disseminated increases in tau-PET signal and validate cut-points for tau-PET. Lastly, our analysis averaged region of interest values from different sides of the brain. In some instances asymmetry in tau-PET signal between sides may exist (Fig. 2) and could be relevant to individual clinical presentations. Further analysis using side-specific tau-PET data and clinical correlation will be needed to assess this observation.

Acknowledgements

We would like to greatly thank AVID Radiopharmaceuticals, Inc., for their support in supplying the AV-1451 precursor, chemistry production advice and oversight, and FDA regulatory cross-filing permission and documentation needed for this work.

Funding

This research was supported by NIH grants, P50 AG016574, R01 NS89757, R01 NS089544, R01 DC10367, U01 AG006786, R21 NS094489, by the Robert Wood Johnson Foundation, The Elsie and Marvin Dekelboum Family Foundation, The Liston Family Foundation and by the Robert H. and Clarice Smith and Abigail van Buren Alzheimer's Disease Research Program, The GHR Foundation, Foundation Dr Corinne Schuler and the Mayo Foundation.

Conflicts of interest

V.J.L consults for Bayer Schering Pharma, Piramal Life Sciences and Merck Research and receives research support from GE Healthcare, Siemens Molecular Imaging, AVID Radiopharmaceuticals and the NIH (NIA, NCI). P.F. receives research support from GE Healthcare, Siemens Molecular Imaging, AVID. B.F.B receives royalties from the publication of Behavioral Neurology of Dementia, serves on the Scientific Advisory Board for the Tau Consortium, and receives research support from GE Healthcare, Axovant Sciences, the NIH, and the Mangurian Foundation. K.A.J. receives research support from the NIH (NIDCD NINDS and NIA). K.K. receives research grants from the NIH/NIA. M.M.Ma. receives research support from the NIH (NIA and NIDCD). M.M.Mi receives research support from the NIH/NIA, Department of Defense, and Biogen and consults for Lysosomal Therapeutics, Inc., and Eli Lilly & Company. R.O.R. receives research support from the NIH and a research grant from F. Hoffman-La Roche. D.S.K. serves on a Data Safety Monitoring Board for Lundbeck Pharmaceuticals and for the DIAN study; is an investigator in clinical trials sponsored by TauRX Pharmaceuticals, Lilly Pharmaceuticals, Biogen and the Alzheimer's Disease Cooperative Study; and receives research support from the NIH. R.C.P. is a consultant for Biogen, Roche, Inc., Merck, Inc. and Genentech, Inc.; receives publishing royalties from Mild Cognitive Impairment (Oxford University Press, 2003), and receives research support from the National Institute of Health. C.R.J. receives research support from the NIH/NIA, and the Alexander Family Alzheimer's Disease Research Professorship of the Mayo Foundation.

H.J.W., M.L.S., S.D.W., T.M.T., M.K.P., M.E.M., D.T.J., P.V., J.G-R. and C.G.S. report no disclosures.

Supplementary material

Supplementary material is available at *Brain* online.

References

American Psychiatric Association. Diagnostic and statistical manual of mental disorders. 4th edn., text revision. Washington, DC: American Psychiatric Association; 2000.

Arriagada PV, Marzloff K, Hyman BT. Distribution of Alzheimer-type pathologic changes in nondemented elderly individuals matches the pattern in Alzheimer's disease. Neurology 1992; 42: 1681–8.

Ashburner J, Friston KJ. Unified segmentation. Neuroimage 2005; 26: 839–51.

Avants BB, Epstein CL, Grossman M, Gee JC. Symmetric diffeomorphic image registration with cross-correlation: evaluating automated labeling of elderly and neurodegenerative brain. Med Image Anal 2008; 12: 26–41.

Bennett DA, Schneider JA, Wilson RS, Bienias JL, Arnold SE. Neurofibrillary tangles mediate the association of amyloid load with clinical Alzheimer disease and level of cognitive function. Arch Neurol 2004; 61: 378–84.

Bouras C, Hof PR, Giannakopoulos P, Michel JP, Morrison JH. Regional distribution of neurofibrillary tangles and senile plaques in the cerebral cortex of elderly patients: a quantitative evaluation of a one-year autopsy population from a geriatric hospital. Cereb Cortex 1994; 4: 138–50.

Braak H, Braak E. Neuropathological stageing of Alzheimer-related changes. Acta Neuropathol 1991; 82: 239–59.

Braak H, Braak E. Frequency of stages of Alzheimer-related lesions in different age categories. Neurobiol Aging 1997; 18: 351–7.

Braak H, Braak E, Bohl J, Reintjes R. Age, neurofibrillary changes, A beta-amyloid and the onset of Alzheimer's disease. Neurosci Lett 1996; 210: 87–90.

Brier MR, Gordon B, Friedrichsen K, McCarthy J, Stern A, Christensen J, et al. Tau and Abeta imaging, CSF measures, and cognition in Alzheimer's disease. Sci Transl Med 2016; 8: 338ra66.

Clark CM, Pontecorvo MJ, Beach TG, Bedell BJ, Coleman RE, Doraiswamy PM, et al. Cerebral PET with florbetapir compared with neuropathology at autopsy for detection of neuritic amyloid-beta plaques: a prospective cohort study. Lancet Neurol 2012; 11: 669–78.

Crary JF, Trojanowski JQ, Schneider JA, Abisambra JF, Abner EL, Alafuzoff I, et al. Primary Age-related Tauopathy (PART): a common pathology associated with human aging. Acta Neuropathol 2014; 128: 755–66.

Driscoll I, Troncoso JC, Rudow G, Sojkova J, Pletnikova O, Zhou Y, et al. Correspondence between in vivo (11)C-PiB-PET amyloid imaging and postmortem, region-matched assessment of plaques. Acta Neuropathol 2012; 124: 823–31.

Duyckaerts C, Bennecib M, Grignon Y, Uchihara T, He Y, Piette F, et al. Modeling the relation between neurofibrillary tangles and intellectual status. Neurobiol Aging 1997; 18: 267–73.

Fawaz MV, Brooks AF, Rodnick ME, Carpenter GM, Shao X, Desmond TJ, et al. High affinity radiopharmaceuticals based upon lansoprazole for PET imaging of aggregated tau in Alzheimer's disease and progressive supranuclear palsy: synthesis, preclinical evaluation, and lead selection. ACS Chem Neurosci 2014; 5: 718–30.

Gertz HJ, Xuereb J, Huppert F, Brayne C, McGee MA, Paykel E, et al. Examination of the validity of the hierarchical model of neuropathological staging in normal aging and Alzheimer's disease. Acta Neuropathol 1998; 95: 154–8.

Gertz HJ, Xuereb JH, Huppert FA, Brayne C, Kruger H, McGee MA, et al. The relationship between clinical dementia and neuropathological staging (Braak) in a very elderly community sample. Eur Arch Psychiatry Clin Neurosci 1996; 246: 132–6.

Guo JL, Lee VM. Seeding of normal Tau by pathological Tau conformers drives pathogenesis of Alzheimer-like tangles. J Biol Chem 2011; 286: 15317–31.

Hashimoto H, Kawamura K, Igarashi N, Takei M, Fujishiro T, Aihara Y, et al. Radiosynthesis, photoisomerization, biodistribution, and metabolite analysis of 11C-PBB3 as a clinically useful PET probe for imaging of tau pathology. J Nucl Med 2014; 55: 1532–8.

Jack CR Jr, Wiste HJ, Weigand SD, Rocca WA, Knopman DS, Mielke MM, et al. Age-specific population frequencies of cerebral beta-amyloidosis and neurodegeneration among people with normal cognitive function aged 50-89 years: a cross-sectional study. Lancet Neurol 2014; 13: 997–1005.

Jack CR Jr, Wiste HJ, Weigand SD, Therneau TM, Lowe VJ, Knopman DS, et al. Defining imaging biomarker cut points for brain aging and Alzheimer's disease. Alzheimers Dement 2017; 13: 205–16.

Johnson KA, Gregas M, Becker JA, Kinnecom C, Salat DH, Moran EK, et al. Imaging of amyloid burden and distribution in cerebral amyloid angiopathy. Ann Neurol 2007; 62: 229–34.

Johnson KA, Schultz A, Betensky RA, Becker JA, Sepulcre J, Rentz D, et al. Tau positron emission tomographic imaging in aging and early Alzheimer disease. Ann Neurol 2016; 79: 110–19.

Josephs KA, Murray ME, Tosakulwong N, Whitwell JL, Knopman DS, Machulda MM, et al. Tau aggregation influences cognition

and hippocampal atrophy in the absence of beta-amyloid: a clinico-imaging-pathological study of primary age-related tauopathy (PART). Acta Neuropathol 2017; 133: 705–15.

Kantarci K, Yang C, Schneider JA, Senjem ML, Reyes DA, Lowe VJ, et al. Antemortem amyloid imaging and beta-amyloid pathology in a case with dementia with Lewy bodies. Neurobiol Aging 2012; 33: 878–85.

Klunk WE, Engler H, Nordberg A, Wang Y, Blomqvist G, Holt DP, et al. Imaging brain amyloid in Alzheimer's disease with Pittsburgh Compound-B. Ann Neurol 2004; 55: 306–19.

Knopman DS, Jack CR Jr, Wiste HJ, Weigand SD, Vemuri P, Lowe VJ, et al. Brain injury biomarkers are not dependent on beta-amyloid in normal elderly. Ann Neurol 2013; 73: 472–80.

Lowe VJ, Curran G, Fang P, Liesinger AM, Josephs KA, Parisi JE, et al. An autoradiographic evaluation of AV-1451 Tau PET in dementia. Acta Neuropathol Commun 2016; 4: 58.

Lowe VJ, Weigand SD, Senjem ML, Vemuri P, Jordan L, Kantarci K, et al. Association of hypometabolism and amyloid levels in aging, normal subjects. Neurology 2014; 82: 1959–67.

Meltzer CC, Kinahan PE, Greer PJ, Nichols TE, Comtat C, Cantwell MN, et al. Comparative evaluation of MR-based partial-volume correction schemes for PET. J Nucl Med 1999; 40: 2053–65.

Murray ME, Lowe VJ, Graff-Radford NR, Liesinger AM, Cannon A, Przybelski SA, et al. Clinicopathologic and 11C-Pittsburgh compound B implications of Thal amyloid phase across the Alzheimer's disease spectrum. Brain 2015; 138 (Pt 5): 1370–81.

Nelson PT, Alafuzoff I, Bigio EH, Bouras C, Braak H, Cairns NJ, et al. Correlation of Alzheimer disease neuropathologic changes with cognitive status: a review of the literature. J Neuropathol Exp Neurol 2012; 71: 362–81.

Okamura N, Harada R, Furumoto S, Arai H, Yanai K, Kudo Y. Tau PET imaging in Alzheimer's disease. Curr Neurol Neurosci Rep 2014; 14: 500.

Ossenkoppele R, Pijnenburg YA, Perry DC, Cohn-Sheehy BI, Scheltens NM, Vogel JW, et al. The behavioural/dysexecutive variant of Alzheimer's disease: clinical, neuroimaging and pathological features. Brain 2015; 138 (Pt 9): 2732–49.

Ossenkoppele R, Schonhaut DR, Scholl M, Lockhart SN, Ayakta N, Baker SL, et al. Tau PET patterns mirror clinical and neuroanatomical variability in Alzheimer's disease. Brain 2016; 139 (Pt 5): 1551–67.

Ossenkoppele R, Zwan MD, Tolboom N, van Assema DM, Adriaanse SF, Kloet RW, et al. Amyloid burden and metabolic function in early-onset Alzheimer's disease: parietal lobe involvement. Brain 2012; 135 (Pt 7): 2115–25.

Petersen RC. Mild cognitive impairment as a diagnostic entity. J Intern Med 2004; 256: 183–94.

Pontecorvo MJ, Devous MD Sr, Navitsky M, Lu M, Salloway S, Schaerf FW, et al. Relationships between flortaucipir PET tau binding and amyloid burden, clinical diagnosis, age and cognition. Brain 2017; 140: 748–63.

Roberts RO, Geda YE, Knopman DS, Cha RH, Pankratz VS, Boeve BF, et al. The Mayo Clinic Study of Aging: design and sampling, participation, baseline measures and sample characteristics. Neuroepidemiology 2008; 30: 58–69.

Sabbagh MN, Cooper K, DeLange J, Stoehr JD, Thind K, Lahti T, et al. Functional, global and cognitive decline correlates to accumulation of Alzheimer's pathology in MCI and AD. Curr Alzheimer Res 2010; 7: 280–6.

Scholl M, Lockhart SN, Schonhaut DR, O'Neil JP, Janabi M, Ossenkoppele R, et al. PET imaging of Tau deposition in the aging human brain. Neuron 2016; 89: 971–82.

Schwarz AJ, Yu P, Miller BB, Shcherbinin S, Dickson J, Navitsky M, et al. Regional profiles of the candidate tau PET ligand 18F-AV-1451 recapitulate key features of Braak histopathological stages. Brain 2016; 139 (Pt 5): 1539–50.

Sperling RA, Rentz DM, Johnson KA, Karlawish J, Donohue M, Salmon DP, et al. The A4 study: stopping AD before symptoms begin? Sci Transl Med 2014; 6: 228fs13.

Stancu IC, Vasconcelos B, Ris L, Wang P, Villers A, Peeraer E, et al. Templated misfolding of Tau by prion-like seeding along neuronal connections impairs neuronal network function and associated behavioral outcomes in Tau transgenic mice. Acta Neuropathol 2015; 129: 875–94.

Takeda S, Wegmann S, Cho H, DeVos SL, Commins C, Roe AD, et al. Neuronal uptake and propagation of a rare phosphorylated high-molecular-weight tau derived from Alzheimer's disease brain. Nat Commun 2015; 6: 8490.

Tzourio-Mazoyer N, Landeau B, Papathanassiou D, Crivello F, Etard O, Delcroix N, et al. Automated anatomical labeling of activations in SPM using a macroscopic anatomical parcellation of the MNI MRI single-subject brain. Neuroimage 2002; 15: 273–89.

Vemuri P, Gunter JL, Senjem ML, Whitwell JL, Kantarci K, Knopman DS, et al. Alzheimer's disease diagnosis in individual subjects using structural MR images: validation studies. Neuroimage 2008a; 39: 1186–97.

Vemuri P, Whitwell JL, Kantarci K, Josephs KA, Parisi JE, Shiung MS, et al. Antemortem MRI based STructural Abnormality iNDex (STAND)-scores correlate with postmortem Braak neurofibrillary tangle stage. Neuroimage 2008b; 42: 559–67.

Xia CF, Arteaga J, Chen G, Gangadharmath U, Gomez LF, Kasi D, et al. [(18)F]T807, a novel tau positron emission tomography imaging agent for Alzheimer's disease. Alzheimers Dement 2013a; 9: 666–76.

Xia M, Wang J, He Y. BrainNet viewer: a network visualization tool for human brain connectomics. PLoS One 2013b; 8: e68910.

Zheng WH, Bastianetto S, Mennicken F, Ma W, Kar S. Amyloid beta peptide induces tau phosphorylation and loss of cholinergic neurons in rat primary septal cultures. Neuroscience 2002; 115: 201–11.

Zimmer ER, Leuzy A, Gauthier S, Rosa-Neto P. Developments in Tau PET Imaging. Can J Neurol Sci 2014; 41: 547–53.